

# Eugenol-loaded chitosan nanoparticles: I. Thermal stability improvement of eugenol through encapsulation

Sarekha Woranuch<sup>a,b</sup>, Rangrong Yoksan<sup>a,b,\*</sup>

<sup>a</sup> Department of Packaging and Materials Technology, Faculty of Agro-Industry, Kasetsart University, Bangkok 10900, Thailand

<sup>b</sup> Center for Advanced Studies in Nanotechnology and Its Applications in Chemical, Food and Agricultural Industries, Kasetsart University, Bangkok 10900, Thailand

## ARTICLE INFO

### Article history:

Received 18 May 2012

Received in revised form 7 August 2012

Accepted 25 August 2012

Available online 11 October 2012

### Keywords:

Chitosan

Encapsulation

Eugenol

Nanoparticle

Thermal stability

## ABSTRACT

The objective of the present work was to improve the thermal stability of eugenol by encapsulating into chitosan nanoparticles via an emulsion–ionic gelation crosslinking method. The influences of the initial eugenol content and tripolyphosphate (TPP) concentration on the loading capacity (LC), encapsulation efficiency (EE), morphology and surface charge of the eugenol-loaded chitosan nanoparticles were also investigated. LC and EE tended to increase with increasing initial eugenol content and decreasing TPP concentration. Particles with LC of 12% and EE of 20% exhibited a spherical shape with an average size of less than 100 nm. Thermal stability of the encapsulated eugenol was verified through its extrusion at 155 °C with a model plastic, i.e. thermoplastic flour (TPF). TPF containing encapsulated eugenol showed 8-fold higher remaining eugenol content and 2.7-fold greater radical scavenging activity than that containing naked eugenol. The results suggest the possible use of eugenol-loaded chitosan nanoparticles as antioxidants in bioactive plastics for food packaging.

© 2012 Elsevier Ltd. All rights reserved.

## 1. Introduction

Eugenol (4-allyl-2-methoxyphenol) is a naturally occurring phenolic compound widely used in food, pharmaceutical, cosmetics and active packaging applications, owing to its effective antimicrobial and antioxidant properties (Baskaran, Periyasamy, & Venkatraman, 2010; Devi, Nisha, Sakthivel, & Pandian, 2010). However, most plant-derived bioactive compounds, including eugenol, are highly volatile, unstable, and sensitive to oxygen, light and heat during processing, utilization and storage (Choi, Soottitantawat, Nuchuchua, Min, & Ruktanonchai, 2009; Garg & Singh, 2011; Gaysinsky, Davidson, Bruce, & Weiss, 2005; Mourtzinou, Kalogeropoulos, Papadakis, Konstantinou, & Karathanos, 2008). In recent decades, nanoencapsulation has become a technique of increasing interest since it offers numerous benefits, including ease of handling, enhanced stability, protection against oxidation, retention of volatile ingredients, taste masking, controlled release, consecutive delivery of multiple active ingredients, change in flavor character, long-lasting organoleptic perception, reduced toxic side effects, improved water solubility of hydrophobic ingredients, and enhanced bioavailability and efficacy (Maurer, Fenske, & Cullis, 2001; Nedovic, Kalusevic, Manojlovic, Levic, & Bugarski, 2011; Neethirajan & Jayas, 2011; Sowasod, Nakagawa, Tanthapanichakoon, & Charinpanitkul, 2012). Choi et al.

(2009) revealed that encapsulation of eugenol into polycaprolactone nanoparticles could enhance its stability against light oxidation. Similarly, the endurance to humidity and UV light of other phenolic compounds, such as thymol, cinnamaldehyde, caffeic acid and carvacrol, through encapsulation has also been reported (Coimbra et al., 2011; Ponce Cevallos, Buera, & Elizalde, 2010).

Emulsion–ionic gelation crosslinking is one of the most promising techniques for entrapment of bioactive compounds. It is an easy process – without the necessity of heat application or the utilization of any toxic crosslinking agents – that generates stable nanosized particles (Keawchaoon & Yoksan, 2011). In most cases, chitosan has been used as a wall/shell material to envelop the active compounds, since this cationic polysaccharide can be crosslinked with other substances bearing multiple negative charges. Chitosan has been used as an outer encapsulant material for a variety of drugs, vitamins, proteins, nutrients and phenolic compounds (Hu et al., 2008; Jang & Lee, 2008) due to its non-toxicity, biocompatibility, biodegradability, and ability to form films, gels, beads and particles. However, there are no existing reports on the encapsulation of eugenol using chitosan as an outer shell; also, verification of the improved thermal stability of encapsulated eugenol through a model plastic has not yet been elucidated.

The objective of the present research was thus to improve the thermal stability of a plant-derived bioactive compound, i.e. eugenol, by encapsulation in chitosan-tripolyphosphate (TPP) nanoparticles. The influence of initial eugenol content and TPP concentration on loading capacity, encapsulation efficiency,

\* Corresponding author. Tel.: +66 2 562 5097; fax: +66 2 562 5046.

E-mail addresses: [rangrong.y@ku.ac.th](mailto:rangrong.y@ku.ac.th), [yrrangrong@yahoo.com](mailto:yrrangrong@yahoo.com) (R. Yoksan).

morphology and surface charge of the particles were determined by UV–vis spectroscopy, Fourier transform infrared spectroscopy (FTIR), thermogravimetric analysis/derivative thermal gravimetric analysis (TGA/DTG), transmission electron microscopy (TEM), dynamic light scattering (DLS), and zeta potential measurement. The thermal stability of eugenol encapsulated in chitosan nanoparticles, as compared with naked eugenol, was also estimated from the remaining content of eugenol and its radical scavenging activity after undergoing a thermal process with a model bioplastic.

## 2. Experimental

### 2.1. Materials

Chitosan (degree of deacetylation of 0.95 and molecular weight of ~760 kDa) was purchased from Seafresh Chitosan (Lab) Co. Ltd., Thailand. Eugenol (99%) and 2,2-diphenyl-1-picrylhydrazyl (DPPH) were obtained from Sigma–Aldrich, Germany. Pentasodium tripolyphosphate (TPP) and Tween 60 were supplied by Fluka Chemika, Switzerland. Acetic acid, hydrochloric acid and ethanol (95%) were purchased from Merck, Germany. Rice flour and waxy rice flour were acquired from Cho Heng Rice Vermicelli Factory Co. Ltd., Thailand. Cassava starch was supplied by Tong Chan Co. Ltd., Thailand.

### 2.2. Preparation of eugenol-loaded chitosan nanoparticles

Eugenol-loaded chitosan nanoparticles were prepared by a two-step method, i.e. oil-in-water (o/w) emulsion and ionic gelation of chitosan with TPP, as described previously (Keawchaon & Yoksan, 2011). Chitosan solution (1.2% w/v) was prepared by agitating chitosan flakes in an aqueous acetic acid solution (1% v/v) at ambient temperature overnight. Tween 60 (0.3 g; hydrophilic–lipophilic balance = 14.9) was added to the chitosan solution (40 mL), and the mixture was stirred at 50 °C for 30 min to obtain a homogeneous solution. Eugenol was gradually dropped into the stirred mixture, and agitation was carried out for 20 min. The content of eugenol was varied (0, 0.12, 0.24, 0.36, 0.48 and 0.60 g) to obtain different weight ratios of chitosan to eugenol (1:0, 1:0.25, 1:0.50, 1:0.75, 1:1.00 and 1:1.25, respectively). TPP solution (40 mL) was slowly dropped into an o/w emulsion while stirring at ambient temperature, and agitation was continuously done for 30 min. The concentration of TPP was also varied: 0.5% (w/v) and 1.0% (w/v). The formed particles were collected by centrifugation at 10,000 rpm for 10 min at 25 °C, and subsequently washed with water several times. The obtained wet particles were dispersed in distilled water (25 mL) and kept at 4 °C. Some of the particles were dried at ambient temperature under reduced pressure and stored in dry conditions at 25 °C.

### 2.3. Characterization of eugenol-loaded chitosan nanoparticles

UV–vis absorption spectra were recorded over a wavelength range of 250–350 nm by a Spectronic Helios Gamma spectrometer (Thermo Electron, USA). FTIR spectra were obtained with a Tensor 27 (Bruker, Germany) using 16 scans at a resolution of 4 cm<sup>−1</sup> over a wavenumber range of 400–4000 cm<sup>−1</sup>. Thermogravimetric analysis (TGA) was performed using a TGA/DSC 1 STARe (Mettler–Toledo, Switzerland) from 25 to 600 °C at a heating rate of 10 °C min<sup>−1</sup> and a nitrogen flow rate of 50 mL min<sup>−1</sup>. TEM micrographs were obtained using a Hitachi H-7650 (Hitachi High-Technologies Corp., Japan) at an accelerating voltage of 100 kV. A drop of the diluted sample dispersion (in water) was deposited directly onto a copper grid and dried under reduced pressure at ambient temperature overnight prior to TEM observation. Hydrodynamic diameter and zeta potential of the particles were analyzed at 20 °C using a Zetasizer Nano ZS model 3600 (Malvern Instruments Ltd., UK) equipped with a He–Ne

laser operating at 4.0 mW and 633 nm with a fixed scattering angle of 90°.

### 2.4. Determination of encapsulation efficiency and loading capacity of eugenol-loaded chitosan nanoparticles

A sample dispersion (in water, 100 µL) was mixed with hydrochloric acid solution (1 M, 5 mL) and boiled at 95 °C for 30 min. Ethanol (1 mL) was then added to the homogeneous mixture before centrifugation at 9000 rpm for 1 min at 25 °C. The supernatant was analyzed by UV–vis spectrophotometry over a wavelength range of 250–350 nm, in which covers a maximum absorption wavelength of eugenol (~283.5 nm) (Shinde & Nagarsenker, 2011). Encapsulation efficiency (EE) and loading capacity (LC) of eugenol were calculated from Eqs. (1) and (2), respectively (Keawchaon & Yoksan, 2011):

$$\%EE = \left( \frac{\text{weight of loaded eugenol}}{\text{weight of initial eugenol}} \right) \times 100 \quad (1)$$

$$\%LC = \left( \frac{\text{weight of loaded eugenol}}{\text{weight of sample}} \right) \times 100 \quad (2)$$

### 2.5. Determination of oxidative stability of eugenol-loaded chitosan nanoparticles

The oxidative stability of naked eugenol and encapsulated eugenol (into chitosan nanoparticles) was studied by a differential scanning calorimetry (DSC). Sample was packed in a DSC aluminum pan with a closed lid having 1-mm-diameter hole at the center. The measurement of oxidation onset temperature was performed using a differential scanning Mettler Toledo DSC 822 calorimeter (Switzerland) from 30 to 400 °C with a heating rate of 10 °C min<sup>−1</sup> and an oxygen flow rate of 50 mL min<sup>−1</sup>.

### 2.6. Preparation of thermoplastic flour containing eugenol-loaded chitosan nanoparticles

Mixed flour (cassava flour/rice flour/waxy rice flour at 50:30:20 w/w/w), glycerol (30%, w/w), and eugenol-loaded chitosan nanoparticles (6%, w/w, corresponding to eugenol content of 0.7%, w/w) were blended in a twin-screw extruder (LTE-20-40; Labtech Engineering Co. Ltd., Thailand) at a temperature range of 95–155 °C. The extrudates were cut using a LZ-120 pelletizer (Labtech) to obtain 3-mm-long pellets. The obtained thermoplastic flour (TPF) containing eugenol-loaded chitosan nanoparticles was dried in a hot-air oven at 45 °C and stored in dry conditions at 25 °C.

TPFN was also prepared using the above protocol without the addition of eugenol-loaded chitosan nanoparticles. In the same way, TPF containing eugenol and TPF containing chitosan nanoparticles were fabricated by adding free eugenol (0.7%, w/w) and chitosan nanoparticles (6%, w/w), respectively, instead of incorporating the eugenol-loaded chitosan nanoparticles.

### 2.7. Determination of remaining eugenol content of thermoplastic flour

TPF (10 mg) was mixed with hydrochloric acid solution (2 M, 5 mL) and boiled at 95 °C for 30 min. After cooling to room temperature, ethanol (1 mL) was added to the homogeneous mixture. The mixture was agitated by a vortex and then centrifuged at 9000 rpm for 2 min at 25 °C. The supernatant was analyzed by a UV–vis spectrophotometer over a wavelength range of 250–350 nm. The remaining content of eugenol was calculated from Eq. (3):

$$X = 24.86Y \quad (R^2 = 0.9949) \quad (3)$$

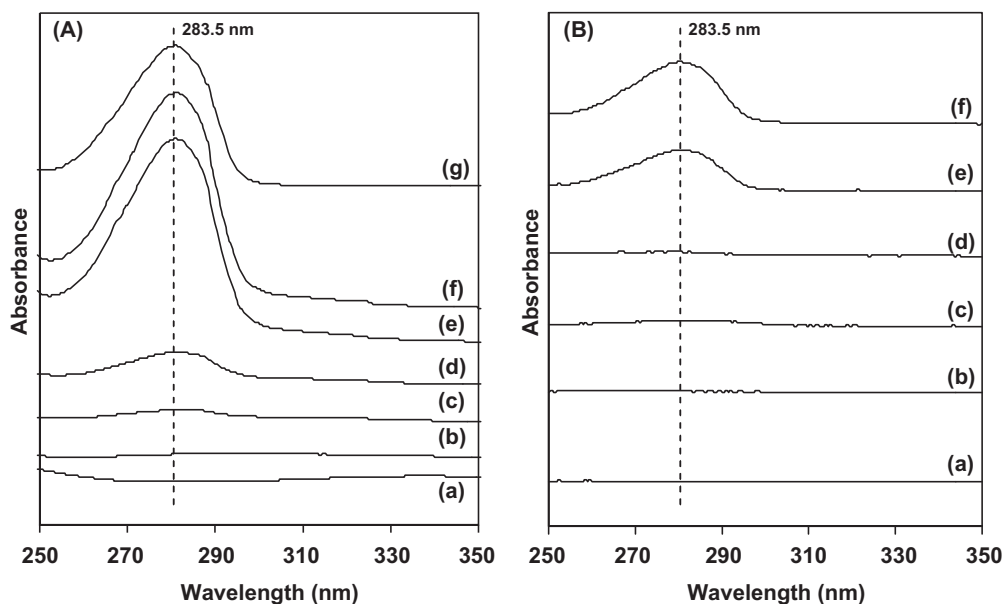


**Fig. 1.** UV–vis absorption spectra of (a) chitosan nanoparticles, (b–f) eugenol-loaded chitosan nanoparticles prepared using different TPP concentrations: (A) 0.5% (w/v) and (B) 1.0% (w/v), with various initial weight ratios of chitosan to eugenol: (b) 1:0.25, (c) 1:0.50, (d) 1:0.75, (e) 1:1 and (f) 1:1.25, and (g) eugenol.

where  $X$  is the remaining content of eugenol (mg/g) and  $Y$  is the absorbance at 283.5 nm of the supernatant in the sample tube. TPFN and TPF containing chitosan nanoparticles were used as blanks for TPF containing free eugenol and TPF containing eugenol-loaded chitosan nanoparticles, respectively.

### 2.8. Antioxidant properties of thermoplastic flour containing eugenol-loaded chitosan nanoparticles

Antioxidant properties of TPF containing free eugenol and TPF containing eugenol-loaded chitosan nanoparticles were assayed by a modified DPPH method reported by Parejo et al. (2002). Briefly, a sample (10 mg) was immersed in an ethanolic solution of stable DPPH radicals (100  $\mu$ M, 100  $\mu$ L) and then incubated in the dark for 2 h. The absorbance of the DPPH solution was then measured at 517 nm. TPFN and TPF containing chitosan nanoparticles were used as blanks for TPF containing free eugenol and TPF containing eugenol-loaded chitosan nanoparticles, respectively. The radical scavenging activity was defined as a decrease in the absorbance of DPPH and was calculated using Eq. (4):

$$\% \text{DPPH decoloration} = \frac{A_{\text{control}} - A_{\text{sample}}}{A_{\text{control}}} \times 100 \quad (4)$$

where  $A_{\text{control}}$  is the absorbance of the supernatant in a control tube and  $A_{\text{sample}}$  is the absorbance of the supernatant in a sample tube.

## 3. Results and discussion

### 3.1. Preparation and characterization of eugenol-loaded chitosan nanoparticles

Eugenol-loaded chitosan nanoparticles were prepared through the formation of oil-in-water emulsion droplets followed by the solidification of the eugenol droplets via ionic gelation of the surrounding chitosan with TPP. The loading of eugenol into chitosan nanoparticles was confirmed by UV–vis spectroscopy, FTIR and TGA/DTG techniques. Chitosan nanoparticles and eugenol-loaded chitosan nanoparticles were digested in hydrochloric acid solution (1 M) at 95 °C to break up the nanoparticles and allow the release of encapsulated eugenol. The supernatant of chitosan

nanoparticles and eugenol-loaded chitosan nanoparticles prepared using a weight ratio of chitosan to eugenol of 1:0.25, exhibited no absorption peak at any wavelength ranging from 250 to 350 nm (Fig. 1a and b). However, the supernatant of eugenol-loaded chitosan nanoparticles prepared using weight ratios of chitosan to eugenol of 1:0.5, 1:0.75, 1:1 and 1:1.25 had a maximum absorption peak at 283.5 nm (Fig. 1c–f), which corresponded to the  $\lambda_{\text{max}}$  of eugenol (Fig. 1g). This result indicated the creation of eugenol-loaded chitosan nanoparticles.

The content of eugenol loaded into the nanoparticles was determined based on the absorbance at 283.5 nm. The LC of eugenol in nanoparticles prepared using a TPP crosslinking agent concentration of 0.5% (w/v) was in the range of 0.85–12.8% when the initial eugenol content ranged from 25 to 125% (w/w) of chitosan (Table 1). This result implied that 100 g of the nanoparticles contained 0.85–12.8 g of eugenol. The LC increased with increasing initial eugenol content. The augmentation of LC as a function of initial bioactive substance content was in agreement with previous studies related to the loading of bovine serum albumin (BSA) and ammonium glycyrrhizinate into chitosan–TPP nanoparticles (Wu, Yang, Wang, Hu, & Fu, 2005; Xu & Du, 2003). Although eugenol-loaded chitosan nanoparticles prepared using a TPP concentration of 1.0% (w/v) showed the same trend of LC increments as a function of initial eugenol content as in the case of those prepared using a TPP concentration of 0.5% (w/v), the calculated LC was lower (Table 1). This suggested that the higher the amount of crosslinking agent used, the lower the LC that would be obtained: a result which might be explained by the increased particle mass. These findings corresponded to those reported by Ajun, Yan, Li, and Huili (2009). Another reason might involve the particle shrinkage caused by high level of crosslink; as a result certain extent of encapsulated eugenol was squeezed out during the particle formation.

Encapsulation efficiency (EE) of nanoparticles prepared using 0.5% (w/v) of TPP was in the range of 2.4–20.2% (Table 1), implying that the amount of loaded eugenol was in the range of 2.4–20.2 g when an initial eugenol content of 100 g was used. Although the EE tended to increase with increasing initial eugenol content, the maximum EE value was obtained for the sample prepared using a weight ratio of chitosan to eugenol of 1:1 (20.2%). A further decrease of EE when the initial eugenol content was 125%

**Table 1**Loading capacity (LC) and encapsulation efficiency (EE) of eugenol determined by UV–vis spectroscopy and intensity ratio of  $I_{2925}/I_{891}$  determined by FTIR technique.

Chitosan:eugenol (w/w)	LC <sup>a</sup> (%)		EE <sup>a</sup> (%)		$I_{2925}/I_{891}$ <sup>b</sup>
	0.5% (w/v) TPP	1.0% (w/v) TPP	0.5% (w/v) TPP	1.0% (w/v) TPP	
1:0.00	0	0	0	0	1.79
1:0.25	n.d.	n.d.	n.d.	n.d.	1.80
1:0.50	0.85 ± 0.01	0.40 ± 0.03	2.36 ± 0.23	1.11 ± 0.09	2.25
1:0.75	2.20 ± 0.71	0.54 ± 0.03	4.44 ± 0.84	1.16 ± 0.07	2.61
1:1.00	11.69 ± 0.14	3.95 ± 0.04	20.17 ± 0.24	6.76 ± 0.80	3.28
1:1.25	12.80 ± 0.24	4.37 ± 0.16	16.85 ± 0.22	5.66 ± 0.20	2.85

<sup>a</sup> Data are reported as mean ± SD ( $n = 3$ ); n.d. = not detected.<sup>b</sup>  $I_{2925}/I_{891}$  represents the intensity ratio of the C–H stretching band at 2925 cm<sup>−1</sup> to the pyranose band at 891 cm<sup>−1</sup>.

(w/w) of chitosan might be explained by the loading limitation. These findings seem to be in accordance with previous studies (Jang & Lee, 2008; Keawchaoon & Yoksan, 2011). These reports disclosed that the EE of ascorbic acid, probucol and carvacrol in chitosan–TPP nanoparticles increased when the initial content of active substances increased up to 21, 16 and 100% (w/w) of chitosan, respectively, while further increased concentration resulted in EE reduction. Similar to the LC result, particles prepared using 1.0% (w/v) of TPP possessed lower EE (1.11–5.66%) than those prepared using 0.5% (w/v) of TPP (Table 1). The reduction of EE might be explained by the shrinkage of the particle shell due to higher crosslinking degree; as a result, the core substance was squeezed out during particle formation. Recently, the EE of catechin was also found to decrease with increasing TPP concentration (Wisuttiprot, Somsiri, Ingkaninan, & Waranuch, 2011). The above results suggested that a weight ratio of chitosan to eugenol of 1:1 and a TPP concentration of 0.5% (w/v) were optimal for the preparation of eugenol-loaded chitosan nanoparticles in the present work.

FTIR is a technique for identifying the chemical composition of a material. Chitosan nanoparticles show major characteristic bands at 3442 cm<sup>−1</sup> (OH), 2927 cm<sup>−1</sup> (CH stretching), 1641 cm<sup>−1</sup> (amide I), 1536 cm<sup>−1</sup> (amide II), 1212 cm<sup>−1</sup> (P=O), 1076 cm<sup>−1</sup> (C–O–C), and 891 cm<sup>−1</sup> (pyranose ring) (Fig. 2a) (Bhumkar & Pokharkar, 2006; Zhang, Jin, & Shi, 2008). Eugenol shows characteristic peaks at 3522 cm<sup>−1</sup> (OH), 2841–3004 cm<sup>−1</sup> (C–H stretching), and 1511 cm<sup>−1</sup>, 1611 cm<sup>−1</sup> and 1638 cm<sup>−1</sup> (C=C aromatic ring) (Fig. 2b) (Dhoot, Auras, Rubino, Dolan, & Soto-Valdez, 2009). Although FTIR

spectra of eugenol-loaded chitosan nanoparticles (Fig. 2c–g) were similar to that of chitosan particles (Fig. 2a), the intensity of the C–H stretching band at 2920–2925 cm<sup>−1</sup> increased with increasing initial content of eugenol. The increments of C–H stretching peak intensity might be a result of eugenol encapsulation. This result indicated the existence of eugenol and chitosan in the nanoparticles. It should be pointed out that the significant increase of C–H stretching band intensity of particles prepared using 0.5% (w/v) of TPP might correspond to the high amount of loaded eugenol (LC). Quantitative analysis by FTIR technique is an indirect method of determining the content of eugenol loaded into chitosan nanoparticles. The C–H stretching peak at 2925 cm<sup>−1</sup> and the pyranose peak at 891 cm<sup>−1</sup> were used as representative bands for eugenol and chitosan, respectively. The intensity ratio of the C–H stretching band to the pyranose band ( $I_{2925}/I_{891}$ ) was calculated only for particles prepared using 0.5% (w/v) of TPP (Table 1). Chitosan nanoparticles possessed an  $I_{2925}/I_{891}$  value of 1.79. Eugenol-loaded chitosan nanoparticles with initial eugenol contents of 25–125% (w/w) of chitosan showed  $I_{2925}/I_{891}$  values in the range of 1.80–3.28, which is higher than that of chitosan nanoparticles, reflecting the successful loading of eugenol. The value of  $I_{2925}/I_{891}$  increased with increasing initial eugenol content up to 100% (w/w) of chitosan. This result confirmed that the weight ratio of chitosan to eugenol of 1:1 was optimal for the present research, corresponding to the result obtained from UV–vis spectroscopy.

TGA is a technique in which the mass of a substance is monitored as a function of temperature or time as the sample is subjected to a controlled temperature program in a controlled atmosphere.

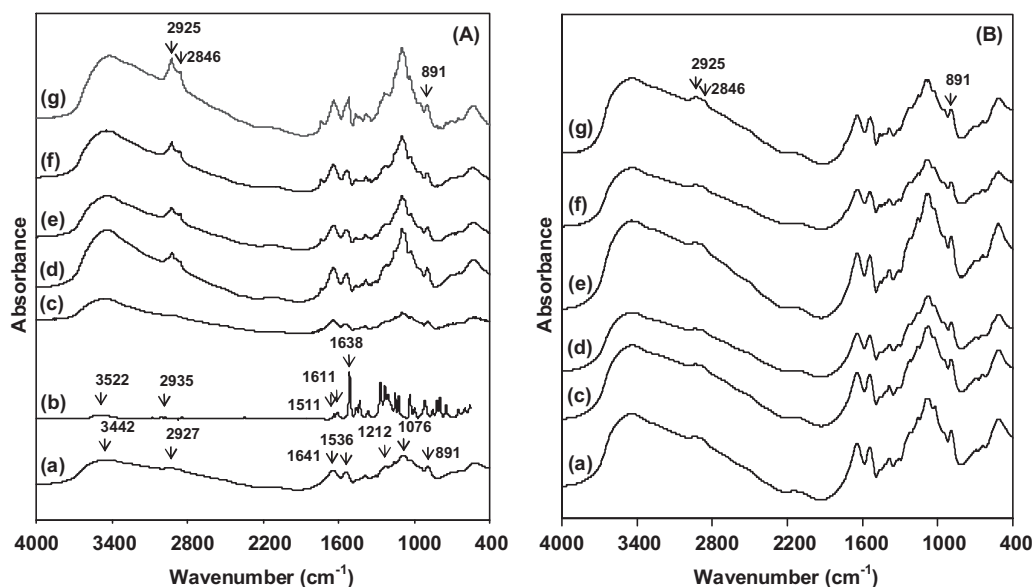


**Fig. 2.** FTIR spectra of (a) chitosan nanoparticles, (b) eugenol, and (c–g) eugenol-loaded chitosan nanoparticles prepared using different TPP concentrations: (A) 0.5% (w/v) and (B) 1.0% (w/v), with various initial weight ratios of chitosan to eugenol: (c) 1:0.25, (d) 1:0.50, (e) 1:0.75, (f) 1:1 and (g) 1:1.25.

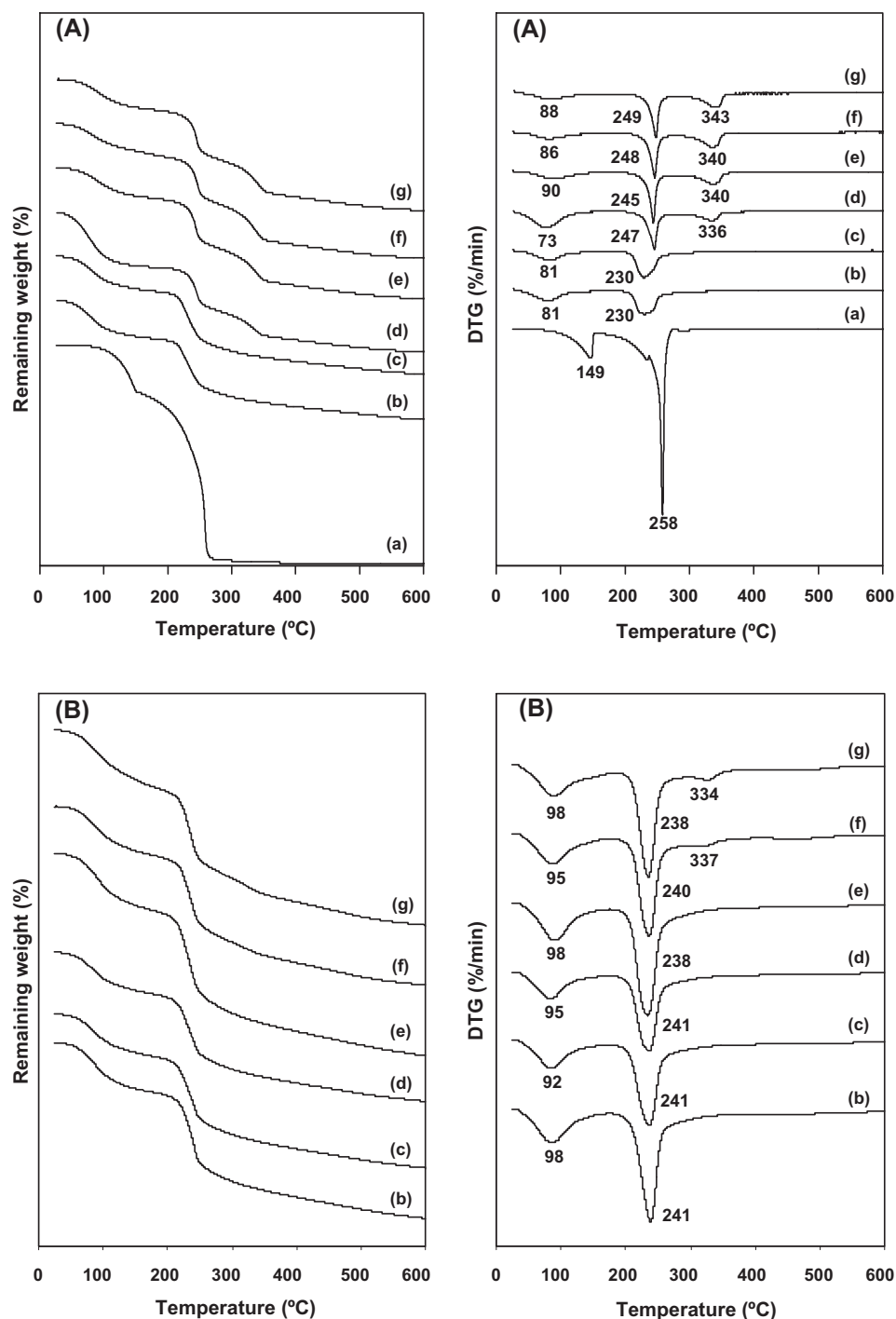


**Fig. 3.** TGA (left) and DTG thermograms (right) of (a) eugenol, (b) chitosan nanoparticles, and (c–g) eugenol-loaded chitosan nanoparticles prepared using different TPP concentrations: (A) 0.5% (w/v) and (B) 1.0% (w/v), with various initial weight ratios of chitosan to eugenol: (c) 1:0.25, (d) 1:0.50, (e) 1:0.75, (f) 1:1.00 and (g) 1:1.25.

The temperature for maximum rate of weight loss was determined as decomposition temperature, which is clearly observed as a peak in the DTG thermogram. Fig. 3 shows that the mass loss of eugenol (Fig. 3Aa), chitosan nanoparticles (Fig. 3b) and eugenol-loaded chitosan nanoparticles (Fig. 3c–g) progresses as a function of temperature. By considering nanoparticles prepared using 0.5% (w/v) of TPP, chitosan nanoparticles and eugenol-loaded chitosan nanoparticles prepared using a weight ratio of chitosan to eugenol of 1:0.25 exhibited two-step mass loss at temperature ranges of 60–110 °C (peak at 80.9 °C) and 210–240 °C (peak

at 230.1 °C) (Fig. 3Ab and c), which might be attributed to the evaporation of moisture and the decomposition of chitosan, respectively (Nam, Park, Ihm, & Hudson, 2010). However, eugenol-loaded chitosan nanoparticles prepared using weight ratios of chitosan to eugenol of 1:0.5, 1:0.75, 1:1 and 1:1.25 presented three-step mass loss at temperature ranges of 30–100 °C (peak at a temperature range from 73 to 90 °C), 230–250 °C (peak at a temperature range from 245 to 249 °C) and 280–340 °C (peak at a temperature range from 336 to 343 °C) (Fig. 3Ad–g). The loss of sample mass at a temperature below 100 °C was related to the liberation



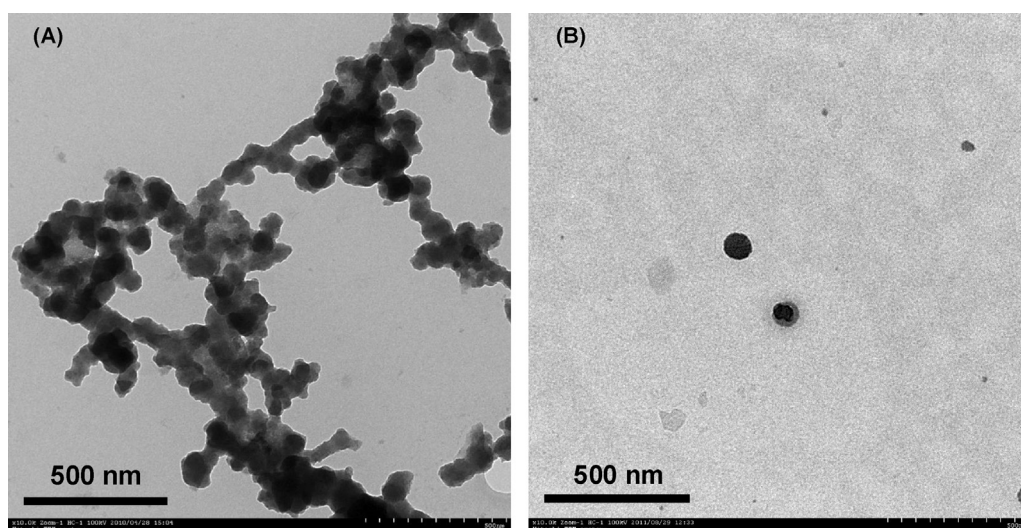


**Fig. 4.** TEM micrographs at 100 kV of eugenol-loaded chitosan nanoparticles prepared using different TPP concentrations: (A) 0.5% (w/v) and (B) 1.0% (w/v), with a weight ratio of chitosan to eugenol of 1:1.

of moisture, while mass loss at mid-temperature could be ascribed to the decomposition of eugenol and chitosan. Mass loss appearing at a temperature above 280 °C might involve the decomposition of encapsulated eugenol. This result revealed the attainment of eugenol-loaded chitosan nanoparticles. It should be pointed out that encapsulated eugenol decomposed at higher temperature than free eugenol, reflecting the improved thermal stability of eugenol by encapsulation into chitosan nanoparticles. Similarly, eugenol-loaded chitosan nanoparticles prepared using 1.0% (w/v) of TPP also showed a two-step mass loss when a low content of eugenol (i.e. 25–75% (w/w) of chitosan) was loaded, and a three-step mass loss when a high content of eugenol (i.e. 100–125% (w/w) of chitosan) was incorporated.

### 3.2. Shape, size and surface charge of eugenol-loaded chitosan nanoparticles

The morphology of the obtained particles was observed by a transmission electron microscope (TEM). Individual eugenol-loaded chitosan nanoparticles exhibited a spherical shape with an average size of 80–100 nm (Fig. 4). The initial content of eugenol did

not significantly influence the shape and size of the nanoparticles (data not shown). However, nanoparticles prepared using 1.0% w/v of TPP formed more perfectly spherical shapes, were a bit larger in size, and showed better dispersibility than nanoparticles prepared using 0.5% (w/v) of TPP (Fig. 4). This might be due to more complete ionic crosslinking. Dynamic light scattering (DLS) technique was also applied to investigate the hydrodynamic diameter of the particles. Fig. 5A shows that the mean diameters of chitosan particles were 586 nm and 683 nm with TPP concentrations used in the preparation step of 0.5% (w/v) and 1.0% (w/v), respectively. The hydrodynamic diameter of the particles became larger when eugenol was loaded: i.e. 723–760 nm and 770–974 nm for particles prepared using 0.5% (w/v) and 1.0% (w/v) of TPP, respectively. The particle diameter tended to slightly increase with increasing initial content of eugenol. The result also reflected that a higher concentration of TPP crosslinking agent produced larger-sized particles, which might be due to the increased crosslinking degree between chitosan and TPP (Ajun et al., 2009). It should be noted that the larger size of particles observed by DLS compared to that by TEM might be a result of swelling and aggregation of the nanoparticles during dispersion in an aqueous medium.

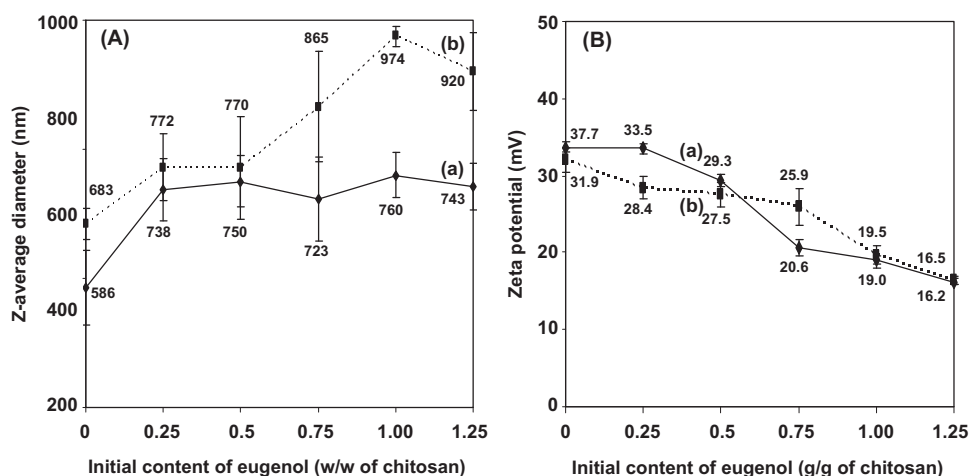


**Fig. 5.** (A) Z-average diameter and (B) zeta potential value of chitosan nanoparticles and eugenol-loaded chitosan nanoparticles prepared using different TPP concentrations: (a) 0.5% (w/v) and (b) 1.0% (w/v), with various initial weight ratios of chitosan to eugenol. Data are reported as mean  $\pm$  SD ( $n = 5$ ).

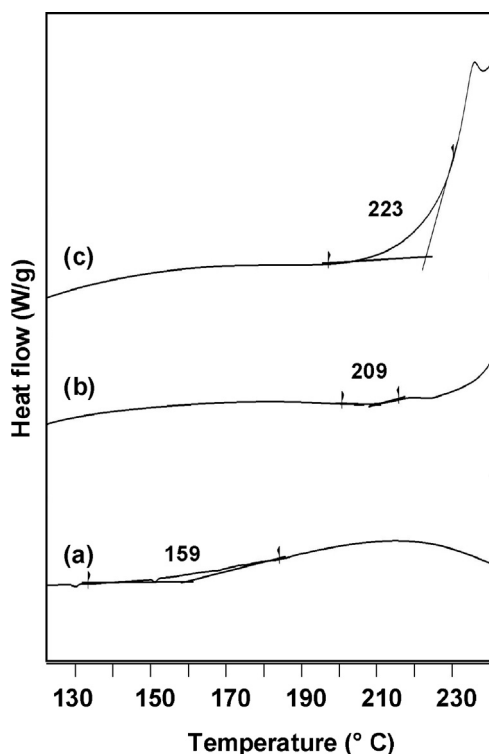


**Fig. 6.** DSC thermograms (exo up) of (a) eugenol, (b) chitosan nanoparticles and (c) eugenol-loaded chitosan nanoparticles prepared using initial weight ratio of chitosan to eugenol of 1:1 and TPP concentration of 0.5% (w/v).

Fig. 5B shows that chitosan nanoparticles prepared using 0.5% (w/v) and 1.0% (w/v) of TPP possess zeta potential values of +37.7 and +31.91 mV, respectively, implying their positively charged surface. The positive surface charge might arise from the protonation of amino groups. With loading of eugenol, zeta potential decreased to values ranging from +16.23 to +33.5 mV for nanoparticles prepared using 0.5% (w/v) of TPP (Fig. 5Ba), and from +16.47 to +28.39 mV for nanoparticles prepared using 1.0% (w/v) of TPP (Fig. 5Bb). The strength of the positive charge at the nanoparticle surface decreased with increasing eugenol content. This might be an effect of charge shielding by migrated and coated eugenol. Some research groups have reported that chitosan–TPP nanoparticles became larger and their zeta potential value decreased when drugs, i.e. ammonium glycyrrhizinate and carvacrol, were incorporated (Keawchaoon & Yoksan, 2011; Wu et al., 2005). They also found that increased drug content caused reduced zeta potential value.

### 3.3. Oxidative stability of eugenol-loaded chitosan nanoparticles

Thermal oxidative stability of the compounds is generally assessed from the exothermal event in DSC thermogram. The oxidative stability of encapsulated eugenol and naked eugenol was investigated by a dynamic oxidation onset temperature method. Eugenol exhibited transition temperature (onset point) at 159 °C reflecting the temperature at which the auto-oxidation process of eugenol began (Fig. 6a). The oxidation reaction of chitosan nanoparticles and eugenol-loaded chitosan nanoparticles started at 209 °C and 223 °C, respectively (Fig. 6b and c). The higher transition temperature of eugenol-loaded chitosan nanoparticles compared with that of chitosan nanoparticles might be a result of antioxidant action of encapsulated eugenol. This result confirmed the existence of eugenol at the temperature above 200 °C, or in other words the

**Table 2**

Remaining content of eugenol and radical scavenging of TPF containing eugenol-loaded chitosan nanoparticles and TPF containing free eugenol.

Sample	Remaining content of eugenol <sup>a</sup> (mg/g)	Radical scavenging <sup>a</sup> (%)
TPF containing free eugenol (0.7%, w/w)	0.033 ± 0.001	14.13 ± 0.20
TPF containing eugenol-loaded chitosan nanoparticles (6%, w/w), corresponding to eugenol content of 0.7% (w/w)	0.303 ± 0.006	52.63 ± 0.46

<sup>a</sup> Data are reported as mean ± SD (n = 3).

improved thermal oxidative stability of eugenol by encapsulating in chitosan nanoparticles.

### 3.4. Remaining eugenol content of thermoplastic flour containing eugenol-loaded chitosan nanoparticles

In order to study the thermal stability of encapsulated eugenol compared with that of naked eugenol, the incorporation of eugenol-loaded chitosan nanoparticles and free eugenol into the model plastic, i.e. thermoplastic flour (TPF) was performed. Herein, eugenol-loaded chitosan nanoparticles prepared from the weight ratio of chitosan to eugenol of 1:1 and TPP concentration of 0.5% (w/v) were chosen because they possessed high LC and EE as well as exhibited small particle size.

The thermal stability of eugenol was estimated from the eugenol content remaining in the TPF, after exposure to heat or after extrusion (a thermal process that involves the forcing of molten material through a die). The remaining content of eugenol was determined by UV–vis spectrophotometry at  $\lambda_{\text{max}}$  of 283.5 nm. After extrusion at temperatures up to 155 °C, TPF containing free eugenol and TPF containing eugenol-loaded chitosan nanoparticles possessed remaining eugenol contents of 0.033 and 0.303 mg/g, respectively (Table 2). The higher amount of eugenol remaining in TPF containing eugenol-loaded chitosan nanoparticles compared to TPF containing free eugenol implied that the encapsulation of eugenol into chitosan nanoparticles could improve the thermal stability of eugenol.

### 3.5. Antioxidant properties of thermoplastic flour containing eugenol-loaded chitosan nanoparticles

Evaluation of the antioxidant activity of eugenol remaining in TPF using a DPPH method is an indirect way of confirming the thermal stability of eugenol. In general, freshly prepared DPPH solution is a deep purple color with a maximum absorption at 517 nm. The antioxidants can quench DPPH free radicals and convert them into a colorless product, resulting in a decrease in absorbance at 517 nm. Table 2 shows that the radical scavenging percentages of TPF containing free eugenol and TPF containing eugenol-loaded chitosan nanoparticles were 14.13 and 52.63%, respectively. This result suggested that TPF containing eugenol-loaded chitosan nanoparticles exhibited 2.7-fold higher antioxidant activity than TPF containing free eugenol. This might be a consequence of the higher remaining content of eugenol in the TPF.

## 4. Conclusions

The aim of this work was to improve the thermal stability of eugenol by encapsulation. Eugenol was encapsulated into chitosan nanoparticles through a two-step method, i.e. the formation of an oil-in-water emulsion and the ionic gelation of emulsion droplets. The obtained particles had loading capacity (LC) and encapsulation efficiency (EE) in the ranges of 0.40–12.8% and 1.1–20.2%,

respectively, with an initial content of eugenol of 50–125% (w/w) of chitosan, and TPP concentrations of 0.5% and 1.0% (w/v). Eugenol-loaded chitosan nanoparticles exhibited a spherical shape with an average individual particle diameter of 80–100 nm and positively charged surface, with a zeta potential value ranging from +16.2 to +33.5 mV. By increasing the initial content of eugenol, the LC, EE and hydrodynamic diameter of the particles tended to increase, while zeta potential value decreased. The augmentation of TPP concentration led to the reduction of LC and EE as well as incremental increases in particle diameter. An initial content of eugenol of 100% (w/w) of chitosan, and a TPP concentration of 0.5% (w/v), were suggested for preparing eugenol-loaded chitosan nanoparticles in the present work. The extrusion of eugenol-loaded chitosan nanoparticles along with thermoplastic flour (TPF), a model plastic, at a temperature up to 155 °C confirmed the improved thermal stability of encapsulated eugenol compared with naked eugenol. TPF containing eugenol-loaded chitosan nanoparticles showed a higher remaining content of eugenol and greater radical scavenging activity than TPF containing free eugenol. These results suggest that eugenol-loaded chitosan nanoparticles could possibly be used as antioxidants for various thermal processing applications, including bioactive plastics for food packaging.

## Acknowledgements

The authors would like to acknowledge the financial support from the Research, Development and Engineering (RD&E) fund through The National Nanotechnology Center (NANOTEC), The National Science and Technology Development Agency (NSTDA), Thailand (Project P-11-00114) to Kasetsart University and the Commission on Higher Education, Ministry of Education, Thailand (National Research University of Thailand). The authors also are grateful to: Prof. Suwabun Chirachanchai, Chulalongkorn University (Thailand), and Hitachi High-Technologies Corporation (Japan) for morphological characterization using a H-7650 TEM; and Mettler-Toledo (Thailand), for its permission in using a TGA instrument.

## References

- Ajun, W., Yan, S., Li, G., & Huili, L. (2009). Preparation of aspirin and probucol in combination loaded chitosan nanoparticles and in vitro release study. *Carbohydrate Polymers*, 75, 566–574.
- Baskaran, Y., Periyasamy, V., & Venkatraman, A. C. (2010). Investigation of antioxidant, anti-inflammatory and DNA-protective properties of eugenol in thioacetamide-induced liver injury in rats. *Toxicology*, 268, 204–212.
- Bhumkar, D. R., & Pokharkar, V. B. (2006). Studies on effect of pH on cross-linking of chitosan with sodium tripolyphosphate: A technical note. *American Association of Pharmaceutical Scientists*, 7, 50.
- Choi, M. J., Soottitantawat, A., Nuchuchua, O., Min, S. G., & Ruktanonchai, U. (2009). Physical and light oxidative properties of eugenol encapsulated by molecular inclusion and emulsion-diffusion method. *Food Research International*, 42, 148–156.
- Coimbra, M., Isacchi, B., van Bloois, L., Torano, J. S., Ket, A., Wu, X., et al. (2011). Improving solubility and chemical stability of natural compounds for medicinal use by incorporation into liposomes. *International Journal of Pharmaceutics*, 416, 433–442.
- Devi, K. P., Nisha, S. A., Sakthivel, R., & Pandian, S. K. (2010). Eugenol (an essential oil of clove) acts as an antibacterial agent against *Salmonella typhi* by disrupting the cellular membrane. *Journal of Ethnopharmacology*, 130, 107–115.
- Dhoot, G., Auras, R., Rubino, M., Dolan, K., & Soto-Valdez, H. (2009). Determination of eugenol diffusion through LLDPE using FTIR-ATR flow cell and HPLC techniques. *Polymers*, 50, 1470–1482.
- Garg, A., & Singh, S. (2011). Enhancement in antifungal activity of eugenol in immunosuppressed rats through lipid nanocarriers. *Colloids and Surfaces B: Biointerfaces*, 87, 280–288.
- Gaybinsky, S., Davidson, P. M., Bruce, B. D., & Weiss, J. (2005). Stability and antimicrobial efficiency of eugenol encapsulated in surfactant micelles as affected by temperature and pH. *Journal of Food Protection*, 68, 1359–1366.
- Hu, B., Pan, C., Sun, Y., Hou, Z., Ye, H., & Zeng, X. (2008). Optimization of fabrication parameters to produce chitosan-tripolyphosphate nanoparticles for delivery of tea catechins. *Journal of Agricultural and Food Chemistry*, 56, 7451–7458.
- Jang, K. I., & Lee, H. G. (2008). Stability of chitosan nanoparticles for L-ascorbic acid during heat treatment in aqueous solution. *Journal of Agricultural and Food Chemistry*, 56, 1936–1941.
- Keawchaoon, L., & Yoksan, R. (2011). Preparation, characterization and in vitro release study of carvacrol-loaded chitosan nanoparticles. *Colloids and Surfaces B: Biointerfaces*, 84, 163–171.
- Maurer, N., Fenske, D. B., & Cullis, P. R. (2001). Developments in liposomal drug delivery systems. *Expert Opinion on Biological Therapy*, 1, 5.
- Mourtzinos, I., Kalogeropoulos, N., Papadakis, S. E., Konstantinou, K., & Karathanos, V. T. (2008). Encapsulation of nutraceutical monoterpenes in  $\beta$ -cyclodextrin and modified starch. *Journal of Food Science*, 73, 89–94.
- Nam, Y. S., Park, W. H., Ihm, D., & Hudson, S. M. (2010). Effect of the degree of deacetylation on the thermal decomposition of chitin and chitosan nanofibers. *Carbohydrate Polymers*, 80, 291–295.
- Nedovic, V., Kalusevic, A., Manojlovic, V., Levic, S., & Bugarski, B. (2011). An overview of encapsulation technologies for food applications. *Procedia Food Science*, 1, 1806–1815.
- Neethirajan, S., & Jayas, D. S. (2011). Nanotechnology for the food and bioprocessing industries. *Food and Bioprocess Technology*, 4, 39–47.
- Parejo, I., Viladomat, F., Bastida, J., Rosas-Romero, A., Flerlage, N., Burillo, J., et al. (2002). Comparison between the radical scavenging activity and antioxidant activity of six distilled and nondistilled Mediterranean herbs and aromatic plants. *Journal of Agricultural and Food Chemistry*, 50, 6882–6890.
- Ponce Cevallos, P. A., Buera, M. P., & Elizalde, B. E. (2010). Encapsulation of cinnamon and thyme essential oils components (cinnamaldehyde and thymol) in  $\beta$ -cyclodextrin: Effect of interactions with water on complex stability. *Journal of Food Engineering*, 99, 70–75.
- Shinde, U., & Nagarsenker, M. (2011). Microencapsulation of eugenol by gelatin-sodium alginate complex coacervation. *Indian Journal of Pharmaceutical Sciences*, 73, 311–315.
- Sowasod, N., Nakagawa, K., Tanthapanichakoon, W., & Charinpanitkul, T. (2012). Development of encapsulation technique for curcumin loaded O/W emulsion using chitosan based cryotropic gelation. *Materials Science and Engineering C*, 32, 790–798.
- Wisutitiprot, W., Somsiri, A., Ingkaninan, K., & Waranuch, N. (2011). A novel technique for chitosan microparticle preparation using a water/silicone emulsion: Green tea model. *International Journal of Cosmetic Science*, 33, 351–358.
- Wu, Y., Yang, W., Wang, C., Hu, J., & Fu, S. (2005). Chitosan nanoparticles as a novel delivery system for ammonium glycyrrhizinate. *International Journal of Pharmaceutics*, 295, 235–245.
- Xu, Y., & Du, Y. (2003). Effect of molecular structure of chitosan on protein delivery properties of chitosan nanoparticles. *International Journal of Pharmaceutics*, 250, 215–225.
- Zhang, Z., Jin, J., & Shi, L. (2008). Antioxidant activity of the derivatives of polysaccharide extracted from a Chinese medical herb (*Ramulus mori*). *Food Science and Technology Research*, 14, 160–168.